Experimental Eye Research 170 (2018) 40–50

Contents lists available at ScienceDirect

Experimental Eye Research

journal homepage: www.elsevier.com/locate/yexer

Nerve fibre layer degeneration and retinal ganglion cell loss long term after optic nerve crush or transection in adult mice☆

M.C. Sánchez-Migallón, F.J. Valiente-Soriano[1], M. Salinas-Navarro[1], F.M. Nadal-Nicolás, M. Jiménez-López, M. Vidal-Sanz**, M. Agudo-Barriuso*

Departamento de Oftalmología, Facultad de Medicina, Universidad de Murcia e Instituto Murciano de Investigación Biosanitaria-VIRGEN DE LA ARRIXACA (IMIB-Arrixaca), Murcia, Spain

ARTICLE INFO

Keywords:
Nerve fiber layer
Optic nerve crush
Optic nerve transection
Brn3a
Antibodies antineurofilaments
Adult albino mice
Retinal nerve fiber layer
Retrograde axonal degeneration
Axotomy
Retinal neurodegeneration

ABSTRACT

We have investigated the long term effects of two different models of unilateral optic nerve (ON) lesion on retinal ganglion cells (RGCs) and their axons, in the injured and contralateral retinas of adult albino mice. Intact animals were used as controls. The left ON was intraorbitally crushed or transected at 0.5 mm from the optic disk and both retinas were analyzed at 2, 3, 5, 7, 14, 30, 45 or 90 days after injury. RGCs were immunoidentified with anti-Brn3a, and their axons with anti-highly phosphorylated axonal neurofilament subunit H (pNFH). After both lesions, RGC death in the injured retinas is first significant at day 3, and progresses quickly up to 7 days slowing down till 90 days. In the same retinas, the anatomical loss of RGC axons is not evident until day 30. However, by two days after both lesions there are changes in the expression pattern of pNFH: axonal beads, axonal club- or bulb-like formations, and pNFH$^+$RGC somas. The number of pNFH$^+$RGC somata peak at day 5 after either lesion and is significantly higher than in intact retinas at all time points. pNFH$^+$RGC somata are distributed across the retina, in accordance with the pattern of RGC death which is diffuse and homogenous. In the contralateral retinas there is no RGC loss, but there are few pNFH$^+$RGCs from day 2 to day 90. In conclusion, in albino mice, axotomy-induced RGC death precedes the loss of their intraretinal axons and occurs in two phases, a rapid and a slower, but steady, one. Injured retinas show similar changes in the pattern of pNFH expression and a comparable course of RGC loss.

1. Introduction

The rodent visual system is widely used to understand the mechanisms underlying neuronal death triggered by axonal injury and/or to test neuroprotective or neuro-regenerative therapies (Aguayo et al., 1987; Avilés-Trigueros et al., 2000; Bray et al., 1991, 1987; Vidal-Sanz et al., 2015, 2002; Valiente-Soriano et al., 2015). In order to evaluate the effects of a treatment it is important to know first the course of degeneration, since this allows to narrow down possible therapeutic windows. Optic nerve (ON) injury, either crush (ONC) or transection (ONT), triggers within a very short period of time the specific and massive death of retinal ganglion cells (RGCs) (Vidal-Sanz et al., 2017; Villegas-Pérez et al., 1993), a response that can be studied *in vivo* to assess the effects of a given neuroprotective treatment (Jehle et al., 2008; Lindqvist et al., 2004; Vidal-Sanz et al., 2000; Parrilla-Reverter et al., 2009a).

In rodents, RGC death after axotomy has been extensively studied by our group (Galindo-Romero et al., 2013a, 2011; Parrilla-Reverter et al., 2009a; Sánchez-Migallón et al., 2016; Villegas-Pérez et al., 1993, reviewed in Vidal-Sanz et al., 2017). In the adult rat, axotomy-induced RGC death occurs in two phases with different kinetics, the first one is quick, and lasts up to 7–9 days, depending on the strain and species (Nadal-Nicolás et al., 2015; Villegas-Pérez et al., 1993), during this first phase ~70–80% of RGCs die. The second phase is slow and steady this is to say that, at least in rat, RGCs die protractedly over 15 months after axotomy (Nadal-Nicolás et al., 2015; Villegas-Pérez et al., 1993). In

☆ Financial support: The Spanish Ministry of Economy and Competitiveness, Instituto de Salud Carlos III, Fondo Europeo de Desarrollo Regional "Una Manera de Hacer Europa" (SAF2015-67643-P, PI16/00031), and Fundación Séneca, Agencia de Ciencia y Tecnología Región de Murcia (19881/GERM/15).

* Corresponding author. Grupo de Oftalmología Experimental, Instituto Murciano de Investigación Biosanitaria-Virgen de la Arrixaca, Edificio LAIB Planta 5a, Carretera Buenavista s/n, 30120, El Palmar, Murcia, Spain.

** Corresponding author. Grupo de Oftalmología Experimental, Instituto Murciano de Investigación Biosanitaria-Virgen de la Arrixaca, Edificio LAIB Planta 5a, Carretera Buenavista s/n, 30120, El Palmar, Murcia, Spain.

E-mail addresses: manuel.vidal@um.es (M. Vidal-Sanz), martabar@um.es (M. Agudo-Barriuso).

[1] Equal contribution.

https://doi.org/10.1016/j.exer.2018.02.010
Received 24 August 2017; Received in revised form 29 January 2018; Accepted 12 February 2018
Available online 13 February 2018

mice, there are no studies spanning longer than 30 days after the lesion (Templeton and Geisert., 2012; Galindo-Romero et al., 2011; Chierzi et al., 1999), thus it is not known whether in mice RGCs die gradually after optic nerve axotomy as observed for rats, or their degeneration halts.

Intra-retinal RGC axons form the retinal nerve fiber layer (RNFL). It has been shown that in rats, ON injury induces changes in the expression pattern of the highly phosphorylated axonal neurofilament subunit H (pNFH) (Dräger and Hofbauer, 1984; Vidal-Sanz et al., 1987; Villegas-Pérez et al., 1988), a protein that is expressed in the mature part of RGC axons in healthy retinas. These changes are typical of RGC degeneration and comprise axonal beads, axonal terminal flares and accumulation of the protein in the RGC somas (Parrilla-Reverter et al., 2009b). Interestingly, in rats, axonal beads are more common after ONT and pNFH$^+$RGC somas after ONC. Furthermore, after ON axotomy the thinning of the RFNL measured *in vivo (*Rovere et al., 2015), and the loss of RGC-axons examined *ex vivo* (Parrilla-Reverter et al., 2009b), occurs later than the loss of RGC somas (Rovere et al., 2015).

In mice Chauhan et al. (2012) using confocal scanning laser ophthalmoscopy (CSLO)/spectral-domain optical coherence tomography (SD-OCT), described that the loss of RGCs was quicker than the reduction of the RFNL during the first 21 days following optic nerve transection. Similarly. Liu et al. (2014) used SD-OCT to analyze the changes in the RFNL from 7 to 28 days after ONC. These *in vivo* tecnhiques have been used as well to monitor the course of RFNL and/or RGC degeneration in other models of retinal injury, such as sustained ocular hypertension (Chen et al., 2015) or partial ONC (Puyang et al., 2016). However, to our knowledge, the *ex vivo* analysis of the anatomical degeneration of the RFNL and its correlation with the death of RGCs long term after both types of axonal injuries, has not been studied in mice. However, it is important to bear in mind that optic nerve injury causes axonal degeneration which is the trigger of RGC death and therefore, precedes the loss of RGC somas. Yet, as the abovementioned studies show, axonal loss occurs later than the loss of the neuronal somas.

Finally, a number of studies have shown that unilateral injury to the retina leads to glial cell alterations in the contralateral, uninjured retina. This phenomenon occurs irrespective of the mechanical or vascular nature of the injury (Bodeutsch et al., 1999; de Hoz et al., 2013; Cen et al., 2015; Galindo-Romero et al., 2013a; Gallego et al., 2012; Kerr et al., 2012; Panagis et al., 2005).

In adult albino mice, using modern techniques to identify and map in retinal whole mounts the general population of RGCs, which can be immunodetected with Brn3a, we have analyzed for the first time following optic nerve transection (ONT) or optic nerve crush (ONC): i) the kinetics of RGC loss from 3 to 90 days after both lesions; ii) the degeneration of the retinal nerve fiber layer in the same retinas, using antibodies against pNFH. This marker was used because changes in its expression pattern are an early sympton of RGC degeneration (Parrilla-Reverter et al., 2009b, and; iii) the effects on the uninjured contralateral retinas, looking for abnormal pNHF expression and/or RGC death. Our results indicate that axotomy-induced RGC death precedes the loss of their intraretinal axons and occurs in two phases, a rapid and a protracted one that lasts up to 90 days. ONT- and ONC-injured retinas show similar changes in the pattern of pNFH expression and a comparable course of RGC loss (a short account of this work has been reported in Abstract form (Sánchez-Migallón et al., 2012)).

2. Material and methods

2.1. Animal handling and surgery

Adult female albino Swiss mice (30 g) were purchased from Charles River (Barcelona Spain) and housed in the animal facilities of the University of Murcia. All animals were treated under protocols approved by European Union guidelines for Animal Care and Use Committee in research and were approved by the Ethical and Animal Studies Committee of the University of Murcia and following the guidelines from Association for Research in Vision and Ophthalmology (ARVO) Statement for the Use of Animals in Ophthalmic and Vision Research.

Animals undergoing surgery were anesthetized by intraperitoneal injection of a mixture of ketamine (60 mg/kg; ketolar, Pfizer, Alcobendas, Madrid, Spain) and xylazine (10 mg/kg; Rompum, Bayer, Kiel, Germany). Analgesia was provided by subcutaneous administration of buprenorphine (0.1 mg/kg; Buprex, Buprenorphine 0.3 mg/mL; Schering-Plough,Madrid, Spain). During and after surgery, the eyes were covered with an ointment (Tobrex; Alcon S. A., Barcelona, Spain) to prevent corneal desiccation.

2.2. Retrograde tracing

After the exposure of both SCi, a pledge of gelatin sponge soaked in 10% hydroxystilbamidine methanesulfonate (OHSt, Molecular Probes, Invitrogen Thermofisher Scientific, Madrid, Spain) dissolved in 10% dimethyl sulfoxide and saline was applied on to both SCi 7 days prior optic nerve injury following standard techniques in our laboratory (Salinas-Navarro et al., 2009).

2.3. Optic nerve injuries

The left optic nerve was crushed or transected at 0.5 mm from the optic disc, respectively, following previously published methods (Galindo-Romero et al., 2013a; Sánchez-Migallón et al., 2016). In brief, to access the optic nerve at the back of the eye, an incision was made in the skin overlying the superior orbital rim, the supero-external orbital contents were dissected, and the superior and external rectus muscles were sectioned. To perform the optic nerve transection, the duramater of the ON was opened longitudinally, and the ON was completely transected. Care was taken not to damage the retinal blood supply. For ONC, the optic nerve was crushed during 10 s using watchmakers forceps. Before and after the procedure, the eye fundus was observed through the operating microscope to assess the integrity of the retinal blood flow. Both retinas of each animal were analyzed, the left retinas (injured ones), and the right uninjured retinas (henceforward contralateral retinas).

2.4. Animal groups

1/Intact, no surgery. **2**/ONC, retinal dissection 2, 3, 5, 7, 14, 30, 45 or 90 days later. **3**/ONT, analyzed at the same time points as before. **4**/RGC tracing, 1 week later ONT, analysis 3 days later; this group was done to verify that pNFH$^+$somas were RGCs. n = 5–6 per group and time point.

2.5. Animal processing, retinal dissection and immunodetection

Unless otherwise stated, all reagents were from Sigma-Aldrich Quimica S.A. Madrid, Spain. Animals were sacrificed with an intraperitoneal injection of an overdose of sodium pentobarbital (Dolethal, Vetoquinol; Especialidades Veterinarias, S.A., Alcobendas, Madrid, Spain). All animals were perfused transcardially with 0.9% saline solution followed by 4% paraformaldehyde in 0.1 M phosphate buffer. Retinas were dissected as flattened whole-mounts as previously described (Salinas-Navarro et al., 2009; Valiente-Soriano et al., 2014).

Double immunodetection was carried out as previously described

(Galindo-Romero et al., 2013a; Parrilla-Reverter et al., 2009b). RGCs were detected using goat α-Brn3a (C-20; Santa-Cruz Biotechnology, Heidelberg, Germany) diluted 1:500. Brn3a is an excellent marker to identify RGCs because its expression declines when the RGC enters in apoptosis (Sánchez-Migallón et al., 2016), thus allowing the identification of injured but viable RGCs. Intra-retinal ganglion cell axons were detected using mouse IgG1 α-highly phosphorylated axonal neurofilament subunit H (pNFH, clone RT-97, MCA1321, Bio-Rad, Bionova Cientifica SL, Madrid, Spain), diluted 1:250. Secondary detection was carried out with donkey α-goat and goat α-mouse IgG1 coupled to Alexa fluor 594 or 488 (Molecular Probes; Thermo Fisher Scientific, Madrid, Spain) diluted at 1:500.

2.6. Image acquisition and analysis

All images were acquired using an epifluorescence microscope (Axioscop 2 Plus; Zeiss Mikroskopie, Jena, Germany) equipped with a computer-driven motorized stage (ProScan H128 Series; Prior Scientific Instruments, Cambridge, UK) controlled by image analysis software (Image-Pro Plus, IPP 5.1 for Windows; Media Cybernetics, Silver Spring, MD). Retinal photomontages were reconstructed from 154 (11 × 14) individual images by zig-zag tiling, as reported (Cuenca et al., 2010; Galindo-Romero et al., 2013a).

The whole population of Brn3a$^+$RGCs was quantified automatically and their distribution assessed by isodensity maps using previously reported methods (Galindo-Romero et al., 2013a, 2011), pNFH$^+$RGC somas were manually dotted on the retinal photomontages, the dots automatically quantified and their distribution visualized using the near neighbour algorithm as reported (Galindo-Romero et al., 2013b; Valiente-Soriano et al., 2014). All maps were plotted using SigmaPlot (SigmaPlot 9.0 for Windows; Systat Software, Inc., Richmond, CA, USA). Finally, using a colour code, these maps depict density of RGCs/mm^2 or the number of neighbours around a cell in a radius of 0.1023 mm.

2.7. Statistical analysis

Data were analyzed and plotted with GraphPad Prism v.7 (GraphPad San Diego, USA). Tests are detailed in results. Differences were considered significant when $p < 0.05$. Data are presented as mean ± standard deviation.

3. Results

3.1. Nerve fiber layer (NFL)

In intact retinas, pNFH expression in the nerve fiber layer (NFL) is circumscribed to the mature portion of RGC axons. Hence, pNFH signal is observed in the central medial retina, along the axonal fascicles that run centripetally from the retinal periphery to converge at the optic disk (Fig. 1A).

After optic nerve injury, either crush or transection, the overall aspect of the NFL appears normal up to 14 days with a density of pNFH$^+$axons that upon inspection under the fluorescent microscope does not appear qualitatively different from intact retinas (Fig. 1). Axonal loss is clear from 30 days onwards. Thus, it is between 14 and 30 days after the ON injury when there is massive clearing of RGC axons, that continues up to 90 days. A this time point, the latest analyzed in this work, some axonal fascicles still remain in the retina.

However, as early as two days after either injury, pNFH expression pattern is subtly altered, indicative of degenerative changes in the RGCs. Firstly, pNFH axonal signal reaches the retinal periphery; secondly pNFH positive somas appear across the retina; and thirdly, later, from day 5 onwards, there are axonal beads and axonal flares strongly pNFH$^+$ (Figs. 1 and 2).

Finally, in contrast to rat (Parrilla-Reverter et al., 2009b) where axonal beads are more abundant after ONT, and pNFH$^+$somas after ONC, in mice there are no clear differences between these two types of injuries.

3.2. RGCs and pNFH$^+$somas

To ascertain whether pNFH$^+$somas are RGCs and not other neurons present in the ganglion cell layer of the mouse retina, we axotomized traced retinas and analyzed them 3 days after the lesion. Brn3a expression in RGCs decreases when the neuron enters in apoptosis (Sánchez-Migallón et al., 2016, 2011), but the tracer will disappear from the RGC after microglial clearance by phagocytosis, an event that is delayed with respect to the actual death of RGCs (Galindo-Romero et al., 2013a; Nadal-Nicolás et al., 2009). Of note, retinas were analyzed 3 days after the injury because at this time point RGC death is already significant (see below Galindo-Romero et al., 2013a; Sánchez-Migallón et al., 2016) and although transcellularly-labelled phagocytic microglial cells have started to appear, they are still few (Galindo-Romero et al., 2013a). As it is shown in Fig. 3, some pNFH$^+$somas express Brn3a to varying degrees while some do not, but all pNFH$^+$somas have the tracer in their cytoplasm demonstrating that indeed correspond to injured RGCs (henceforward pNFH$^+$RGCs).

3.3. Contralateral retinas

The right, uninjured fellow retinas were also analyzed. In Figs. 1B and 4 is shown that the aspect of the NFL and the density of RGCs in a right retina analyzed 90 days after crushing the left ON does not differ from intact retinas. After a closer inspection, we did find pNFH$^+$RGCs in all of the contralateral retinas, but only in 2 of the 6 intact retinas analyzed (Table 1, Fig. 4). In fact, the number of pNFH$^+$RGCs in the contralateral retinas is significantly higher than in intact ones at all time points and after both lesions. Because pNFH accumulation in the RGC somas is an early symptom of degeneration, we quantified in the same retinas the numbers of Brn3a$^+$RGCs. In the contralateral uninjured retinas (Table 1, Fig. 4**),** although their mean number diminished slightly, there were no statistically significant decreases in the total numbers of Brn3a$^+$RGCs up to 90 days.

3.4. Injured retinas

As above mentioned, in the injured retinas the loss of central pNFH$^+$axons is not evident until 30 days after either lesion (Figs. 1, 5 and 6). In the same retinas, pNFH$^+$RGCs appear already at day 2, scattered across the retina (Table 1, Figs. 5 and 6). Their number increases up to day 5, declining thereafter. Nevertheless, pNFH$^+$RGCs are significantly more abundant than in intact or contralateral retinas at all time points analyzed. Concomitantly, Brn3a$^+$RGCs disappear from the retina homogeneously. RGC loss is first significant at day 3 (15–20% of the original population), and by day 7, approximately 62–65% have died. Then, RGC death slows down, and during the next week a further 15% dies. At day 30, 6–7% of RGCs survive and thereafter, while there is not a significant decrease of RGCs, 16–20% of the RGCs remaining at 30 days are lost at 90 days. At this latest time point, with only approximately 5% of RGC survival, some isolated axonal bundles are still present in the central retina. Again, there were no differences between

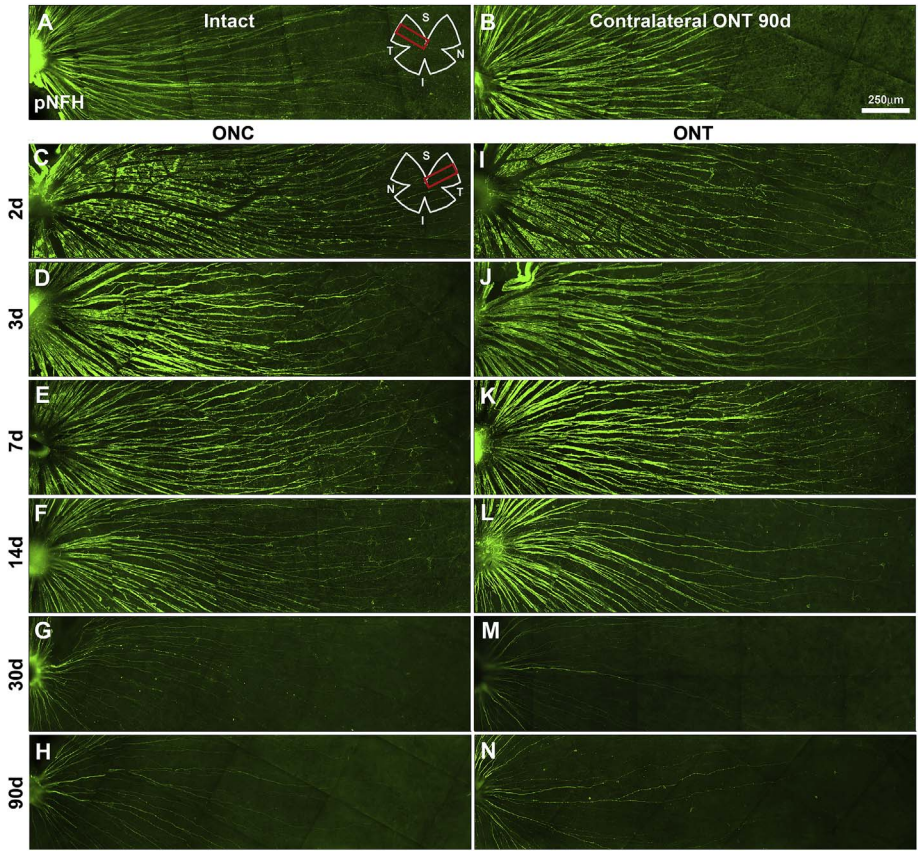

Fig. 1. Temporal degeneration of the nerve fiber layer in the retina after optic nerve axotomy.
Magnifications from flatmounted retinas taken from the dorso-temporal quadrant (red frame in the retinal schemes in A and C) showing the aspect of the nerve fiber layer (pNFH immunodetection) in a representative intact retina (**A**), in a contralateral to an injured one analyzed 90 days after ONT (**B**), and in injured retinas analyzed at increasing time points after ONC (**C-H**) or ONT (**I-J**). In all images the optic nerve head is to the left. S: superior, I: inferior. T: temporal. N: nasal. d: days.

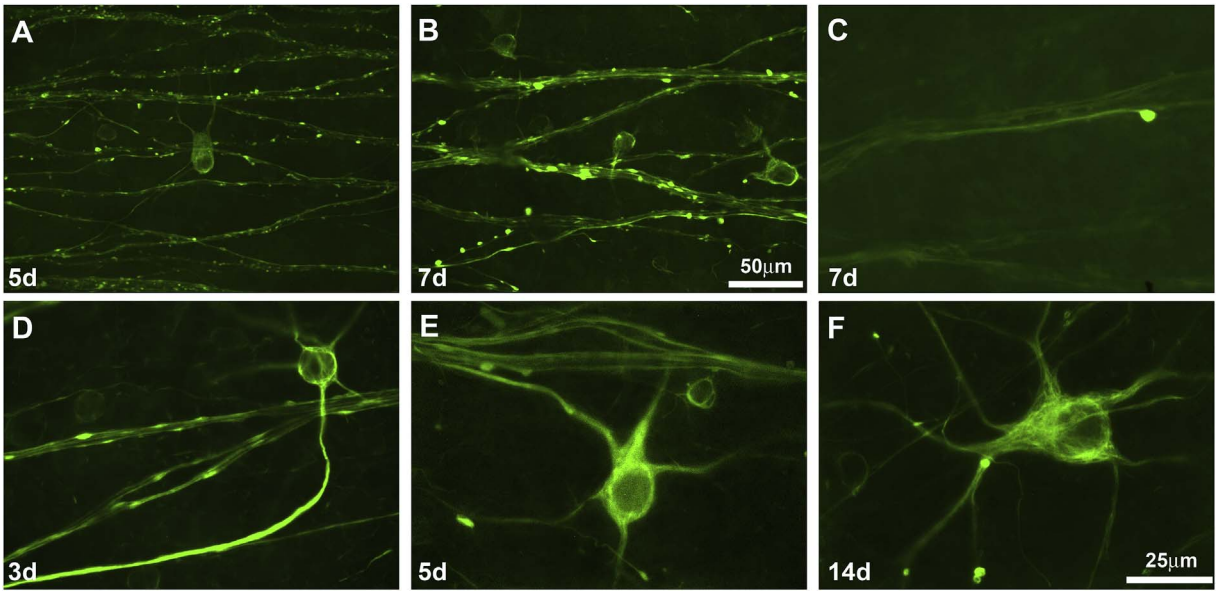

Fig. 2. Changes in the expression pattern of pNFH after optic nerve axotomy.
Magnifications showing the main alterations observed in pNFH expression after ONC or ONT: beaded axons (**A-B**), axons ending in flare like shapes (**C**), and pNFH$^+$somas (**A,B, D-F**). d: days after the injury. Scale bars for A-C in **B**, and for D-F in panel **F**.

both optic nerve injuries.

4. Discussion

Here we show for the first time a comparative study of the loss of RGCs and their axons up to 90 days after two different ON lesions in the adult albino mice. As shown for the albino rat (Nadal-Nicolás et al., 2015; Villegas-Pérez et al., 1993), albino mice RGC loss follows also two kinetics after ON injury: during the first 7 days, almost 70% of the original RGC population is lost (present results and Galindo-Romero

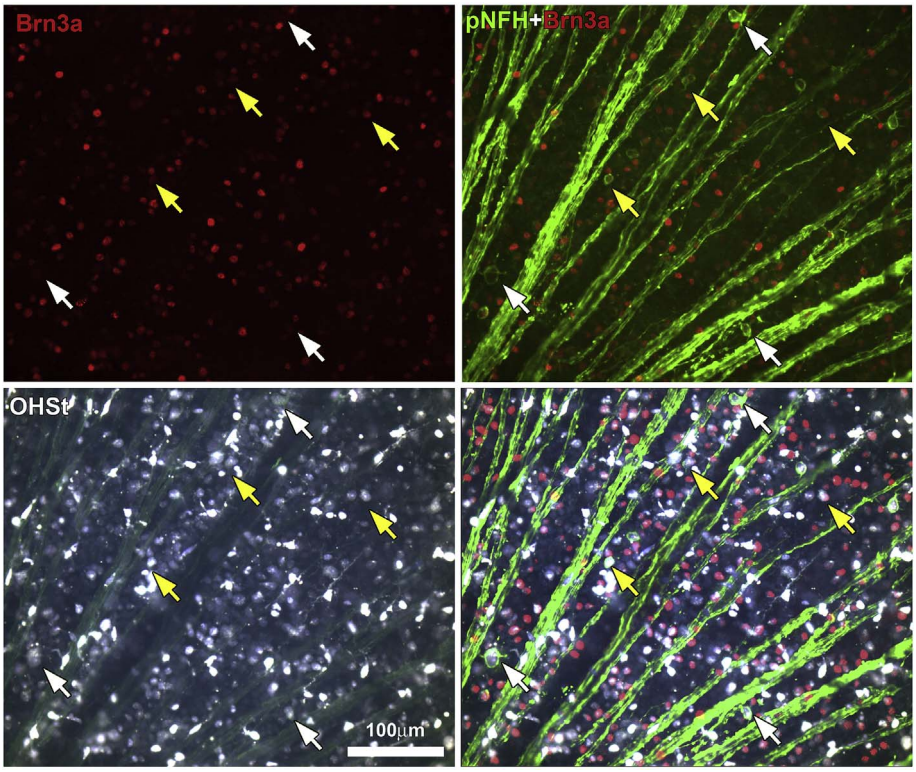

Fig. 3. Upon axotomy, pNFH locates in the somas of injured RGCs.
Magnification from a traced flat mounted retina analyzed 3 days after ONT, showing Brn3a and pNFH immunodetection, and OHSt tracing. Yellow arrows point to RGC somas with accumulation of pNFH, that still express Brn3a, and white ones to those that do not express Brn3a anymore.

et al., 2011; Sánchez-Migallón et al., 2016), reaching 85% a week later and from then onwards RGC death continues very slowly and steadily at least until 90 days (the latest point analyzed here).

While RGC loss was evident by day 3 after ON injury, a clear diminution in axonal density was not observed in the whole mounts until 30 days, when approximately over 90% of the RGC population is already lost. The temporal disparity between the loss of RGC somas and their intraretinal axons following intraorbital ON axotomy is in agreement with our previous studies in adult rats (Rovere et al., 2015) and with works in mice (Chauhan et al., 2012; Munguba et al., 2014) that show, using *in vivo* approaches, that the reduction of the RFNL lags behind the loss of RGCs. Furthermore, this shift has been reported as well after ocular hypertension induced by laser photocoagulation of the episcleral and perilimbal veins, an injury that results in an axotomy-like damage to RGC axons at the level of the ON head (Salinas-Navarro et al., 2010; Vidal-Sanz et al., 2015).

Here, we have observed, using pNFH as axonal marker, that qualitatively there is not a clear loss of intraretinal axons during the first 14 days, a time frame during which 85% of RGCs have died. However, from 14 to 30 days, with the exception of isolated fascicles, most RGC axons disappeared. Why is there such a mismatch between the rapid RGC disappearance and the more protracted degeneration of the intraretinal axons? At present we do not have a clear explanation, but it is possible that Brn3a expression vanishes when the RGC enters in apoptosis, while pNFH is an structural protein that will remain in the cell until it is cleared by microglial phagocytosis. This correlates with the fact that traced-RGCs somas are seen in the tissue longer than Brn3a signal (Galindo-Romero et al., 2013a; Nadal-Nicolás et al., 2009). Retrogradely labelled RGCs disappear from the tissue much earlier than the pNFH axonal signal (Parrilla-Reverter et al., 2009b); clearing dead somas is probably more urgent than clearing the axons since the release of cytoplasmic content into the tissue would harm the surrounding displaced amacrine cells (Diaz-Aparicio et al., 2016).

Interestingly, pNFH expression pattern changes at 2 days, the earliest time point that we analyzed, in accordance with the fact that axonal degeneration is the biological event that precedes soma loss. The first observed change is pNFH reaching the peripheral retina and pNFH accumulation in the RGC somas. Both indicate that the cellular mechanisms controlling compartmentalization are damaged, suggesting an impaired cellular homeostasis. In agreement with it, most of the pNFH$^+$RGC either do not express Brn3a or express lower quantities which concords with the fact that Brn3a expression declines when the RGC expresses the cleaved form of caspase 3 (c-casp3, Sánchez-Migallón et al., 2016). Furthermore, there is a temporal parallelism between the course of c-casp3 expression and the appearance of pNFH$^+$RGCs, with only two differences, i/c-casp3$^+$RGCs peak at 4 days, and pNFH$^+$RGCs at day 5 (although here we have not studied 4 days after the lesion) and ii/more pNFH$^+$RGCs than c-casp3$^+$RGCs are immunodetected at a given time point. Again, this may be a reflection of the functional characteristics of both proteins, since c-casp3 has a transient expression that will only be detected during a very brief time window while pNFH will stay until microglial clearance. Overall, our

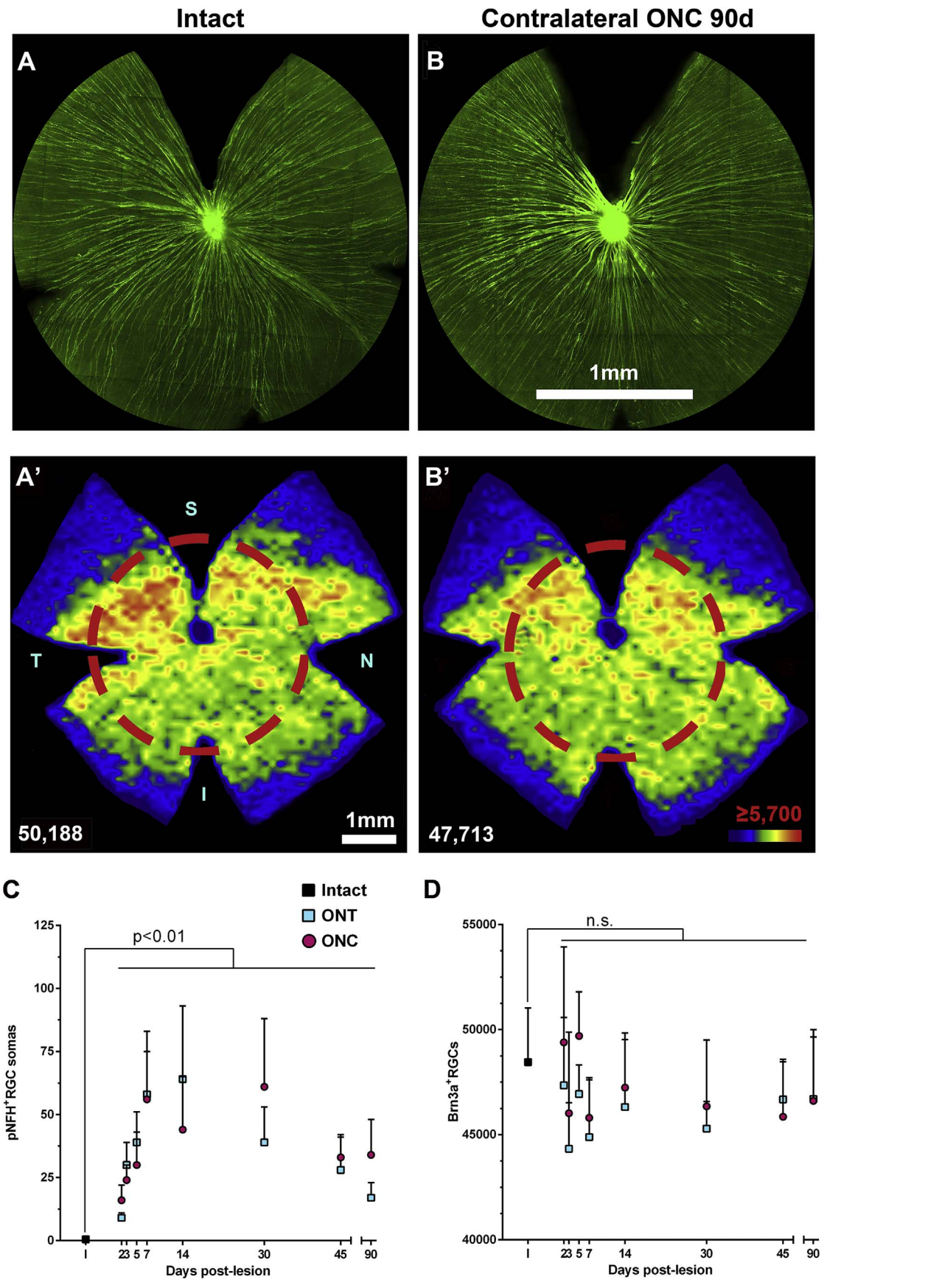

(caption on next page)

Fig. 4. Nerve fiber layer and RGCs in intact and contralateral retinas.
A–B: Magnifications from the central retina (red circles in A′-B′) showing RGC axons (pNFH immunodetection) converging to the optic head in an intact (A) and in a right retina 90 days after crushing the left optic nerve (contralateral retina) (B). A′-B': isodensity maps showing the distribution of RGCs in these same retinas. Isodensity maps illustrate the density (number of cells/mm^2) with a colour scale that goes from 0 RGCs/mm^2 (purple) to ≥5700 RGCs/mm^2 (red). Below each map is shown the number of RGCs quantified in their corresponding retina. S: superior, I: inferior, N: nasal, T: temporal C: X,Y graph showing the mean number + standard deviation of pNFH$^+$RGCs in intact and contralateral retinas at increasing times post-lesion. D: X,Y graph showing the mean number + standard deviation of Brn3a$^+$RGCs in the same retinas as C. Multiple comparison Kruskal-Wallis test and Dunn's post-hoc test for pNFH$^+$RGCs and ANOVA and Tukey's post-hoc test for Brn3a$^+$RGCs. n.s. no significant difference (for detailed statistics, see Table 1).

Table 1
Number of Brn3a$^+$RGCs and pNFH$^+$RGCs somas in intact, contralateral, and injured retinas.

Intact (n = 6)	pNFH$^+$RGCs				Brn3a$^+$RGCs			
	0.5 ± *0.5*				48,451 ± *2584*			
	ONC				ONT			
	Contralateral		*Injured*		*Contralateral*		*Injured*	
Days post-lesion	pNFH$^+$ RGCs	Brn3a$^+$ RGCs	pNFH$^+$ RGCs	Brn3a$^+$ RGCs	pNFH$^+$ RGCs	Brn3a$^+$ RGCs	pNFH$^+$ RGCs	Brn3a$^+$ RGCs
2	16 ± *5*††	49,396 ± *4538*	550††† ± *141*	44,415 ± *4315*	9 ± *2*††	47,351 ± *3228*	477††† ± *135*	46,100 ± *3824*
3	24 ± *6**††††	46,019 *3862*	1263*** ± *227*	40,815† ± *6807*	30 ± *9*††††	44,327 ± *2200*	1164*** ± *88*	39,073†† ± *3438*
5	30 ± *13*	49,697 ± *2096*	2264*** ± *318*	29,501*** ± *4989*	39 ± 12	46,938 ± *1375*	2056*** ± *394*	29,999*** ± *4604*
7	56 ± *27**	45,802 ± *1812*	795*** ± *141*	18,829*** ± *2310*	58 ± *17**	44,882 ± *2835*	791*** ± *125*	17,245*** ± *1517*
14	44 ± *21*	47,238 ± *2606*	870 ± *212*	10,741*** ± *1536*	64 ± *29*	46,318 ± *3206*	868 ± *160*	9835*** ± *2601*
30	61 ± *27*	46,348 ± *3159*	347*** ± *103*	3181*** ± *542*	39 ± *14**	45,292 ± *1292*	264*** ± *139*	3350** ± *855*
45	33 ± *8**	45,855 ± *2614*	527 ± *167*	3009 ± *1262*	28 ± *14*	46,679 ± *1906*	412 ± *76*	2937 ± *817*
90	33 ± *14*	46,609 ± *3382*	174 ± *56*	2539 ± *811*	17 ± *6*	46,700 ± *2952*	222 ± *100*	2813 ± *858*

Data are presented as the mean ± *standard deviation*. In the contralateral retinas, the number of RGCs does not differ from intact retinas ($p > 0.05$ Kruskal-Wallis and Dunn's post-hoc test). There are no differences between ONC or ONT at any time point. In the injured retinas, the decrease of RGCs is first statistically significant at 3 days progressing significantly up to 30 days. Thereafter and up to 90 days, the number of RGCs decreases but does not reach statistical significance. In the contralateral and injured retinas, there is a significant increase at all time points of pNFH$^+$somas compared to intact retinas ($p < 0.01$). Statistics for pNFH$^+$RGCs Kruskal-Wallis and Dunn's post-hoc test and for Brn3a$^+$RGCs ANOVA and Tukey's post-hoc. †Significant compared to intact retinas (†$p < 0.05$, ††$p < 0.01$, †††$p < 0.001$).*Significant compared to the previous time point (*$p < 0.05$, **$p < 0.01$, ***$p < 0.001$). ONC: optic nerve crush. ONT: optic nerve transection. n = 5–6 retinas per group and time point.

data indicate that when pNFH translocates to the RGC somas, the neuron is in an impaired cellular homeostasis.

We have observed a previously unreported contralateral response to optic nerve injury that involves the expression of pNFH in RGCs, but without a statistical decrease in the total numbers of RGCs in these right retinas. pNFH$^+$RGCs in the right untouched retina were fairly constant and scattered throughout, reminiscent of the contralateral phagocytic microglial response observed in this species and strain (Galindo-Romero et al., 2013a). This observation adds to the biological effect of retinal injury on the contralateral fellow retina (Bodeutsch et al., 1999; de Hoz et al., 2013; Cen et al., 2015; Galindo-Romero et al., 2013a; Gallego et al., 2012; Kerr et al., 2012; Panagis et al., 2005), but at present we have no clear explanation for this observation.

In rat, ONC and ONT induce a different course of RGC loss (Nadal-Nicolas et al., 2015) which is not observed in mice (this work, and Sánchez-Migallón et al., 2016). We think that the different course of RGC loss between species and injuries may be due to the distance from the ON head at which the lesions were performed while in rat ONC was done at 3 mm and ONT at 0.5 mm, in mice both lesions have been carried out at 0.5 mm.

Regarding the pattern of pNFH abnormalities, there are differences between ONC and ONT in rats, but not in mice. Indeed, in rat pNFH$^+$RGC somas are more frequent after ONC than ONT. In this case, the distance to the lesion site is the same for both lesions but differs between species: 3 mm in rats (Parrilla-Reverter et al., 2009b) and 0.5 mm in the current study. Thus, there are two possible explanations, either pNFH changes are related to the distance itself, and/or to the species, and so rats respond differently to both lesions irrespectively of the distance. Injuring the mice optic nerve at 3 mm would shed some light into this.

5. Conclusions

In mice RGC loss after axotomy continues, albeit slowly, up to 90 days after the lesion. Our results demonstrate a mismatch between the early onset of RGC disappearance and the more protracted degeneration of the intraretinal RGC axons. ONT- and ONC-injured retinas show similar changes in the pattern of pNFH expression and a comparable course of RGC loss.

Finally, immunodetection of pNFH might be suitable as a marker of RGC stress in therapeutic studies that assess neuroprotection/neuroregeneration, because it labels the somas of unhealthy RGCs not only in acute studies but also in chronic ones.

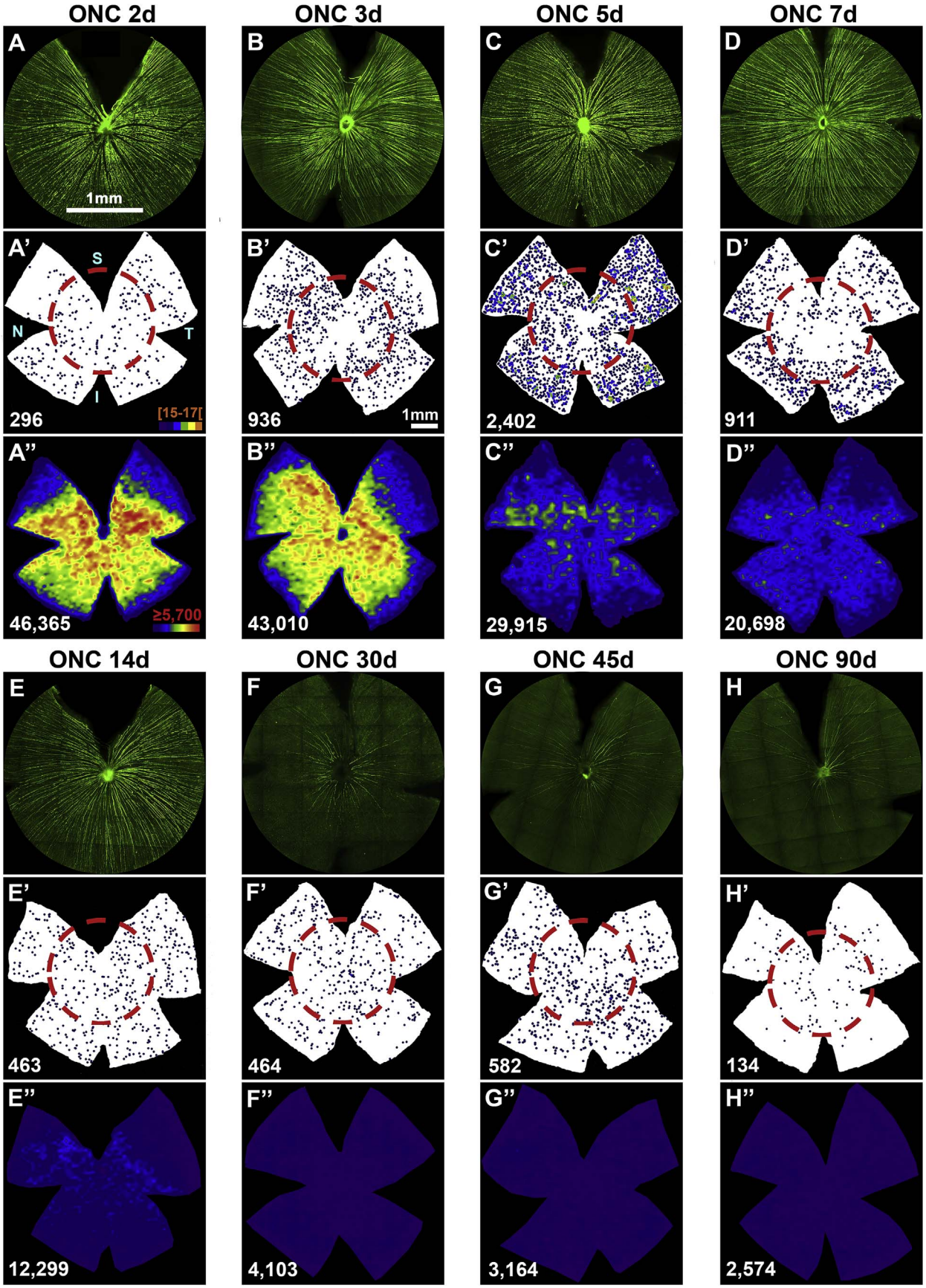

Fig. 5. Topographical loss of intraretinal axons and RGCs, and appearance of pNFH$^+$RGC somas after ONC.
A–H: Magnifications from the central retina (red circles in A′-H′) showing RGC axons (pNFH immunodetection) converging to the optic head in retinas analyzed at increasing times after ONC. In these same retinas, the number and distribution of pNFH$^+$RGCs (A′-H′) and surviving Brn3a$^+$RGCs (A″-H″) was assessed. A′-H': neighbour maps. A″-H'': isodensity maps. Colour scale for isodensity maps goes from 0 RGCs/mm^2 (purple) to ≥5700 RGCs/mm^2 (red) and for neighbour maps from 0 to 1 (purple) to ≥8–9 (bright green) neighbours. Below each map is shown the number of RGCs or pNFH$^+$RGCs quantified in their corresponding retina. S: superior, I: inferior, N: nasal, T: temporal.

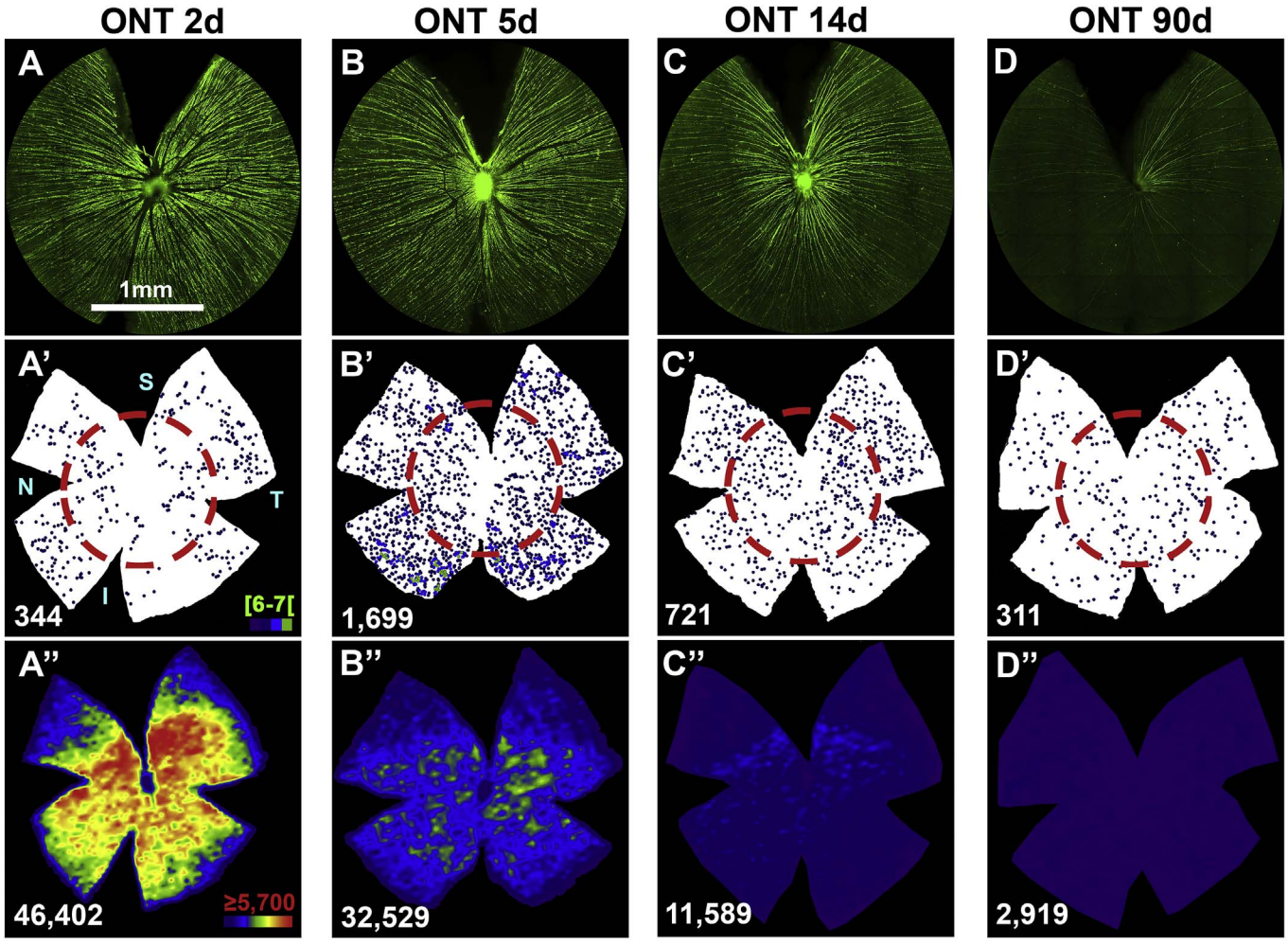

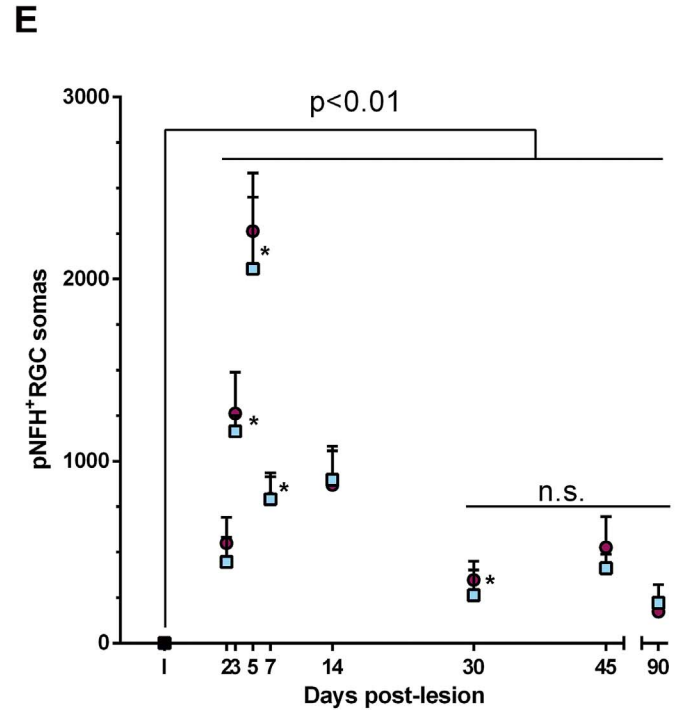

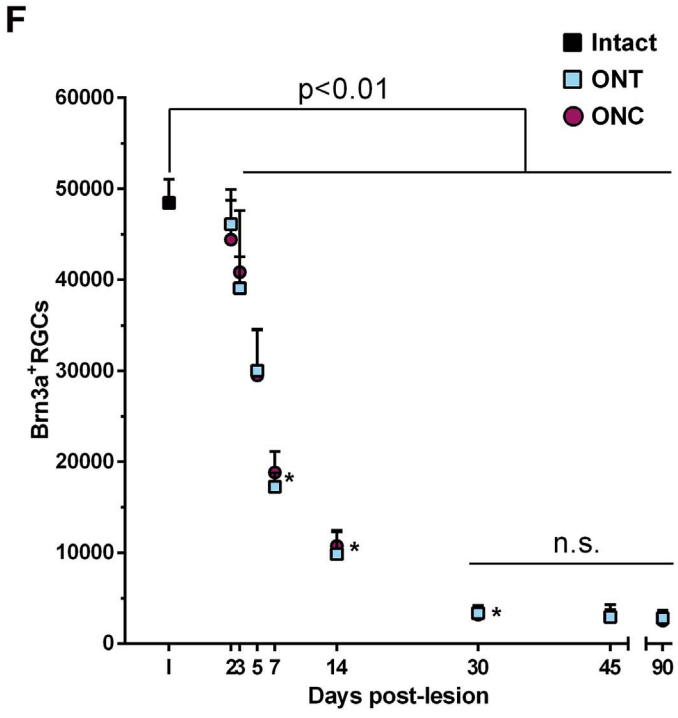

(caption on next page)

Fig. 6. Topographical loss of intraretinal axons and Brn3a$^+$RGCs, and appearance of pNFH$^+$RGC somas after ONT. Quantitative analysis.
A–D: Magnifications from the central retina (red circles in A′-D′) showing RGC axons (pNFH immunodetection) converging to the optic head in retinas analyzed at increasing times after ONT. In these same retinas, the number and distribution of pNFH$^+$RGCs (A′-D′) and surviving Brn3a$^+$RGCs (A″-D″) was assessed. A′-D': neighbour maps A″-D": isodensity maps. Colour scale for isodensity maps goes from 0 RGCs/mm^2 (purple) to ≥5700 RGCs/mm^2 (red) and for neighbour maps from 0 to 1 (purple) to ≥6–7 (bright green) neighbours. Below each map is shown the number of RGCs or pNFH$^+$RGCs quantified in their corresponding retina. S: superior, I: inferior, N: nasal, T: temporal. E: X,Y graph showing the mean number + standard deviation of pNFH$^+$RGCs in intact and injured retinas at increasing times post-lesion. D: X,Y graph showing the mean number + standard deviation of Brn3a$^+$RGCs in the same retinas as E. Multiple comparison Kruskal-Wallis test and Dunn's post-hoc test for pNFH$^+$RGCs and ANOVA and Tukey's post-hoc test for Brn3a$^+$RGCs. *Significantly different compared to the previous time point ($p < 0.05$). n.s. no significant difference (for a more detailed statistics see Table 1).

Appendix A. Supplementary data

Supplementary data related to this article can be found at http://dx.doi.org/10.1016/j.exer.2018.02.010.

References

Aguayo, A.J., Vidal-Sanz, M., Villegas-Pérez, M.P., Bray, G.M., 1987. Growth and connectivity of axotomized retinal neurons in adult rats with optic nerves substituted by PNS grafts linking the eye and the midbrain. Ann. N. Y. Acad. Sci. 495, 1–9.

Avilés-Trigueros, M., Sauvé, Y., Lund, R.D., Vidal-Sanz, M., 2000. Selective innervation of retinorecipient brainstem nuclei by retinal ganglion cell axons regenerating through peripheral nerve grafts in adult rats. J. Neurosci. 20, 361–374.

Bodeutsch, N., Siebert, H., Dermon, C., Thanos, S., 1999. Unilateral injury to the adult rat optic nerve causes multiple cellular responses in the contralateral site. J. Neurobiol. 38, 116–128.

Bray, G.M., Vidal-Sanz, M., Aguayo, A.J., 1987. Regeneration of axons from the central nervous system of adult rats. Prog. Brain Res. 71, 373–379.

Bray, G.M., Villegas-Pérez, M.P., Vidal-Sanz, M., Carter, D.A., Aguayo, A.J., 1991. Neuronal and nonneuronal influences on retinal ganglion cell survival, axonal regrowth, and connectivity after axotomy. Ann. N. Y. Acad. Sci. 633, 214–228.

Cen, L.P., Han, M., Zhou, L., Tan, L., Liang, J.J., Pang, C.P., Zhang, M., 2015. Bilateral retinal microglial response to unilateral optic nerve transection in rats. Neuroscience 311, 56–66.

Chauhan, B.C., Stevens, K.T., Levesque, J.M., Nuschke, A.C., Sharpe, G.P., O'Leary, N., Archibald, M.L., Wang, X., 2012. Longitudinal in vivo imaging of retinal ganglion cells and retinal thickness changes following optic nerve injury in mice. PLoS One 7, e40352.

Chen, H., Zhao, Y., Liu, M., Feng, L., Puyang, Z., Yi, J., Liang, P., Zhang, H.F., Cang, J., Troy, J.B., Liu, X., 2015. Progressive degeneration of retinal and superior collicular functions in mice with sustained ocular hypertension. Invest. Ophthalmol. Vis. Sci. 56, 1971–1984.

Chierzi, S., Strettoi, E., Cenni, M.C., Maffei, L., 1999. Optic nerve crush: axonal responses in wild-type and bcl-2 transgenic mice. J. Neurosci. 19, 8367–8376.

Cuenca, N., Pinilla, I., Fernández-Sánchez, L., Salinas-Navarro, M., Alarcón-Martínez, L., Avilés-Trigueros, M., de la Villa, P., Miralles de Imperial, J., Villegas-Pérez, M.P., Vidal-Sanz, M., 2010. Changes in the inner and outer retinal layers after acute increase of the intraocular pressure in adult albino Swiss mice. Exp. Eye Res. 91, 273–285.

de Hoz, R., Gallego, B.I., Ramírez, A.I., Rojas, B., Salazar, J.J., Valiente-Soriano, F.J., Avilés-Trigueros, M., Villegas-Perez, M.P., Vidal-Sanz, M., Triviño, A., Ramírez, J.M., 2013. Rod-like microglia are restricted to eyes with laser-induced ocular hypertension but absent from the microglial changes in the contralateral untreated eye. PLoS One 8, e83733.

Diaz-Aparicio, I., Beccari, S., Abiega, O., Sierra, A., 2016. Clearing the corpses: regulatory mechanisms, novel tools, and therapeutic potential of harnessing microglial phagocytosis in the diseased brain. Neural Regen Res. 11, 1533–1539.

Dräger, U.C., Hofbauer, A., 1984. Antibodies to heavy neurofilament subunit detect a subpopulation of damaged ganglion cells in retina. Nature 309, 624–626.

Galindo-Romero, C., Avilés-Trigueros, M., Jiménez-López, M., Valiente-Soriano, F.J., Salinas-Navarro, M., Nadal-Nicolás, F., Villegas-Pérez, M.P., Vidal-Sanz, M., Agudo-Barriuso, M., 2011. Axotomy-induced retinal ganglion cell death in adult mice: quantitative and topographic time course analyses. Exp. Eye Res. 92, 377–387.

Galindo-Romero, C., Valiente-Soriano, F.J., Jiménez-López, M., García-Ayuso, D., Villegas-Pérez, M.P., Vidal-Sanz, M., Agudo-Barriuso, M., 2013a. Effect of brain-derived neurotrophic factor on mouse axotomized retinal ganglion cells and phagocytic microglia. Invest. Ophthalmol. Vis. Sci. 54, 974–985.

Galindo-Romero, C., Jiménez-López, M., García-Ayuso, D., Salinas-Navarro, M., Nadal-Nicolás, F.M., Agudo-Barriuso, M., Villegas-Pérez, M.P., Avilés-Trigueros, M., Vidal-Sanz, M., 2013b. Number and spatial distribution of intrinsically photosensitive retinal ganglion cells in the adult albino rat. Exp. Eye Res. 108, 84–93.

Gallego, B.I., Salazar, J.J., de Hoz, R., Rojas, B., Ramírez, A.I., Salinas-Navarro, M., Ortín-Martínez, A., Valiente-Soriano, F.J., Avilés-Trigueros, M., Villegas-Perez, M.P., Vidal-Sanz, M., Triviño, A., Ramírez, J.M., 2012. IOP induces upregulation of GFAP and MHC-II and microglia reactivity in mice retina contralateral to experimental glaucoma. J. Neuroinflammation 9, 92.

Jehle, T., Dimitriu, C., Auer, S., Knoth, R., Vidal-Sanz, M., Gozes, I., Lagrèze, W.A., 2008. The neuropeptide NAP provides neuroprotection against retinal ganglion cell damage after retinal ischemia and optic nerve crush. Graefes Arch. Clin. Exp. Ophthalmol. 246, 1255–1263.

Kerr, N.M., Johnson, C.S., Zhang, J., Eady, E.K., Green, C.R., Danesh-Meyer, H.V., 2012. High pressure-induced retinal ischaemia reperfusion causes upregulation of gap junction protein connexin43 prior to retinal ganglion cell loss. Exp. Neurol. 234, 144–152.

Lindqvist, N., Peinado-Ramón, P., Vidal-Sanz, M., Hallböök, F., 2004. GDNF, Ret, GFRalpha1 and 2 in the adult rat retino-tectal system after optic nerve transection. Exp. Neurol. 187, 487–499.

Liu, Y., McDowell, C.M., Zhang, Z., Tebow, H.E., Wordinger, R.J., Clark, A.F., 2014. Monitoring retinal morphologic and functional changes in mice following optic nerve crush. Invest. Ophthalmol. Vis. Sci. 55, 3766–3774.

Munguba, G.C., Galeb, S., Liu, Y., Landy, D.C., Lam, D., Camp, A., Samad, S., Tapia, M.L., Lee, R.K., 2014. Nerve fiber layer thinning lags retinal ganglion cell density following crush axonopathy. Invest. Ophthalmol. Vis. Sci. 55, 6505–6513.

Nadal-Nicolás, F.M., Jiménez-López, M., Sobrado-Calvo, P., Nieto-López, L., Cánovas-Martínez, I., Salinas-Navarro, M., Vidal-Sanz, M., Agudo, M., 2009. Brn3a as a marker of retinal ganglion cells: qualitative and quantitative time course studies in naive and optic nerve-injured retinas. Invest. Ophthalmol. Vis. Sci. 50, 3860–3868.

Nadal-Nicolás, F.M., Sobrado-Calvo, P., Jiménez-López, M., Vidal-Sanz, M., Agudo-Barriuso, M., 2015. Long-term effect of optic nerve axotomy on the retinal ganglion cell layer. Invest. Ophthalmol. Vis. Sci. 56, 6095–6112.

Panagis, L., Thanos, S., Fischer, D., Dermon, C.R., 2005. Unilateral optic nerve crush induces bilateral retinal glial cell proliferation. Eur. J. Neurosci. 21, 2305–2309.

Parrilla-Reverter, G., Agudo, M., Sobrado-Calvo, P., Salinas-Navarro, M., Villegas-Pérez, M.P., Vidal-Sanz, M., 2009a. Effects of different neurotrophic factors on the survival of retinal ganglion cells after a complete intraorbital nerve crush injury: a quantitative in vivo study. Exp. Eye Res. 89, 32–41.

Parrilla-Reverter, G., Agudo, M., Nadal-Nicolás, F., Alarcón-Martínez, L., Jiménez-López, M., Salinas-Navarro, M., Sobrado-Calvo, P., Bernal-Garro, J.M., Villegas-Pérez, M.P., Vidal-Sanz, M., 2009b. Time-course of the retinal nerve fibre layer degeneration after complete intra-orbital optic nerve transection or crush: a comparative study. Vis. Res. 49, 2808–2825.

Puyang, Z., Feng, L., Chen, H., Liang, P., Troy, J.B., Liu, X., 2016. Retinal ganglion cell loss is delayed following optic nerve crush in NLRP3 knockout mice. Sci. Rep. 6, 20998.

Rovere, G., Nadal-Nicolás, F.M., Agudo-Barriuso, M., Sobrado-Calvo, P., Nieto-López, L., Nucci, C., Villegas-Pérez, M.P., Vidal-Sanz, M., 2015. Comparison of retinal nerve fiber layer thinning and retinal ganglion cell loss after optic nerve transection in adult albino rats. Invest. Ophthalmol. Vis. Sci. 56, 4487–4498.

Salinas-Navarro, M., Alarcón-Martínez, L., Valiente-Soriano, F.J., Ortín-Martínez, A., Jiménez-López, M., Avilés-Trigueros, M., Villegas-Pérez, M.P., de la Villa, P., Vidal-Sanz, M., 2009. Functional and morphological effects of laser-induced ocular hypertension in retinas of adult albino Swiss mice. Mol. Vis. 15, 2578–2598.

Salinas-Navarro, M., Alarcón-Martínez, L., Valiente-Soriano, F.J., Jiménez-López, M., Mayor-Torroglosa, S., Avilés-Trigueros, M., Villegas-Pérez, M.P., Vidal-Sanz, M., 2010. Ocular hypertension impairs optic nerve axonal transport leading to progressive retinal ganglion cell degeneration. Exp. Eye Res. 90, 168–183.

Sánchez-Migallón, M.C., Nadal-Nicolás, F.M., Jiménez-López, M., Sobrado-Calvo, P., Vidal-Sanz, M., Agudo-Barriuso, M., 2011. Brain derived neurotrophic factor maintains Brn3a expression in axotomized rat retinal ganglion cells. Exp. Eye Res. 92, 260–267.

Sánchez-Migallón, M.C., Salinas-Navarro, M., Jiménez-López, M., Nadal-Nicolás, F., Nieto-López, L., Valiente-Soriano, F.J., Sobrado-Calvo, P., Villegas-Pérez, M.P., Vidal-Sanz, M., Agudo-Barriuso, M., 2012. Quantitative and qualitative analyses of the nerve fiber layer degeneration after optic nerve axotomy in adult mice. Invest. Ophthalmol. Vis. Sci. 53 E-Abstract 3488.

Sánchez-Migallón, M.C., Valiente-Soriano, F.J., Nadal-Nicolás, F.M., Vidal-Sanz, M., Agudo-Barriuso, M., 2016. Apoptotic retinal ganglion cell death after optic nerve transection or crush in mice: delayed RGC loss with BDNF or a caspase 3 inhibitor. Invest. Ophthalmol. Vis. Sci. 57, 81–93.

Templeton, J.P., Geisert, E.E., 2012. A practical approach to optic nerve crush in the mouse. Mol. Vis. 18, 2147–2152.

Valiente-Soriano, F.J., García-Ayuso, D., Ortín-Martínez, A., Jiménez-López, M., Galindo-Romero, C., Villegas-Pérez, M.P., Agudo-Barriuso, M., Vugler, A.A., Vidal-Sanz, M., 2014. Distribution of melanopsin positive neurons in pigmented and albino mice: evidence for melanopsin interneurons in the mouse retina. Front. Neuroanat. 8, 131.

Valiente-Soriano, F.J., Nadal-Nicolás, F.M., Salinas-Navarro, M., Jiménez-López, M., Bernal-Garro, J.M., Villegas-Pérez, M.P., Agudo-Barriuso, M., Vidal-Sanz, M., 2015. BDNF rescues RGCs but not intrinsically photosensitive RGCs in ocular hypertensive albino rat retinas. Invest. Ophthalmol. Vis. Sci. 56, 1924–1936.

Vidal-Sanz, M., Bray, G.M., Villegas-Pérez, M.P., Thanos, S., Aguayo, A.J., 1987. Axonal regeneration and synapse formation in the superior colliculus by retinal ganglion cells in the adult rat. J. Neurosci. 7, 2894–2909.

Vidal-Sanz, M., Lafuente, M., Sobrado-Calvo, P., Selles-Navarro, I., Rodriguez, E., Mayor-Torroglosa, S., Villegas-Perez, M.P., 2000. Death and neuroprotection of retinal ganglion cells after different types of injury. Neurotox. Res. 2, 215–227.

Vidal-Sanz, M., Avilés-Trigueros, M., Whiteley, S.J., Sauvé, Y., Lund, R.D., 2002. Reinnervation of the pretectum in adult rats by regenerated retinal ganglion cell

axons: anatomical and functional studies. Prog. Brain Res. 137, 443–452.
Vidal-Sanz, M., Valiente-Soriano, F.J., Ortín-Martínez, A., Nadal-Nicolás, F.M., Jiménez-López, M., Salinas-Navarro, M., Alarcón-Martínez, L., García-Ayuso, D., Avilés-Trigueros, M., Agudo-Barriuso, M., Villegas-Pérez, M.P., 2015. Retinal neurodegeneration in experimental glaucoma. Prog. Brain Res. 220, 1–35.
Vidal-Sanz, M., Galindo-Romero, C., Valiente-Soriano, F.J., Nadal-Nicolás, F.M., Ortin-Martinez, A., Rovere, G., Salinas-Navarro, M., Lucas-Ruiz, F., Sanchez-Migallon, M.C., Sobrado-Calvo, P., Aviles-Trigueros, M., Villegas-Pérez, M.P., Agudo-Barriuso, M., 2017. Shared and differential retinal responses against optic nerve injury and ocular hypertension. Front. Neurosci. 11, 235.
Villegas-Pérez, M.P., Vidal-Sanz, M., Bray, G.M., Aguayo, A.J., 1988. Influences of peripheral nerve grafts on the survival and regrowth of axotomized retinal ganglion cells in adult rats. J. Neurosci. 8, 265–280.
Villegas-Pérez, M.P., Vidal-Sanz, M., Rasminsky, M., Bray, G.M., Aguayo, A.J., 1993. Rapid and protracted phases of retinal ganglion cell loss follow axotomy in the optic nerve of adult rats. J. Neurobiol. 24, 23–36.

Update

Experimental Eye Research
Volume 190, Issue , January 2020, Page

DOI: https://doi.org/10.1016/j.exer.2019.107875

Experimental Eye Research 190 (2020) 107875

Contents lists available at ScienceDirect

Experimental Eye Research

journal homepage: www.elsevier.com/locate/yexer

Corrigendum

Corrigendum to "Nerve fibre layer degeneration and retinal ganglion cell loss long term after optic nerve crush or transection in adult mice" [Exp Eye Res. (2018) 170:40–50. doi: 10.1016/j.exer.2018.02.010. Epub 2018 Feb 13]

M.C. Sánchez-Migallón, F.J. Valiente-Soriano, M. Salinas-Navarro, F.M. Nadal-Nicolás, M. Jiménez-López, M. Vidal-Sanz, M. Agudo-Barriuso*

Departamento de Oftalmología, Facultad de Medicina, Universidad de Murcia, Instituto Murciano de Investigación Biosanitaria-Virgen de la Arrixaca (IMIB-Arrixaca), Murcia, Spain

The authors inform that there was an error in the methods section, in this article the mice were male instead of female.

The authors would like to apologise for any inconvenience caused.

DOI of original article: https://doi.org/10.1016/j.exer.2018.02.010

* Corresponding author. Grupo de Oftalmología Experimental, Instituto Murciano de Investigación Biosanitaria-Virgen de la Arrixaca, Edificio LAIB Planta 5ª, Despacho 5.18, Carretera Buenavista s/n, 30120, El Palmar, Murcia, Spain.

E-mail address: martabar@um.es (M. Agudo-Barriuso).

https://doi.org/10.1016/j.exer.2019.107875

Available online 20 November 2019